NISTIR 6588

FIFTEENTH MEETING OF THE UJNR PANEL ON FIRE RESEARCH AND SAFETY MARCH 1-7, 2000

VOLUME 2

Sheilda L. Bryner, Editor

National Institute of Standards and Technology
Technology Administration, U.S. Department of Commerce

NISTIR 6588

FIFTEENTH MEETING OF THE UJNR PANEL ON FIRE RESEARCH AND SAFETY MARCH 1-7, 2000

VOLUME 2

Sheilda L. Bryner, Editor

November 2000

U. S. Department of Commerce
Norman Y. Mineta, Secretary
Technology Administration
Dr. Cheryl L. Shavers, Under Secretary of Commerce for Technology
National Institute of Standards and Technology
Raymond G. Kammer, Director

Heating, Spalling Characteristics and Residual Properties of High Performance Concrete

Long T. Phan, James R. Lawson, Frank L. Davis
National Institute of Standards and Technology
Building and Fire Research Laboratory

ABSTRACT

This paper describes results of NIST's experimental program to study effects of elevated temperature exposure on residual mechanical properties of high-performance concrete (HPC). The cylindrical test specimens were made from four mixtures with water-to-cementitious material ratio (*w/cm*) ranging from 0.22 to 0.57, and room-temperature compressive strength ranging from 51 MPa to 93 MPa. Two of the mixtures contained silica fume. The specimens were heated to an interior temperature of 450 °C, at a heating rate of 5 °C/min. Elastic modulus and compressive strength were measured after cooling to room temperature. Results indicate that, within the range of compressive strength examined (51 MPa to 93 MPa), HPCs with higher original strength (lower *w/cm*) and with silica fume have higher relative residual strength after elevated temperature exposure than those with lower original strength (higher *w/cm*) and without silica fume. The differences in modulus of elasticity are less significant. However, the potential for explosive spalling increased in HPC specimens with lower *w/cm* and silica fume.

INTRODUCTION

High-performance concrete (HPC) can be manufactured by most concrete plants due to the availability of a variety of additives such as silica fume, fly ash, blast furnace slag, and water reducing admixtures. HPC often offers significant economic, architectural, and structural advantages over conventional concrete, and is being used more widely in structural applications, especially when high durability is desired.

It is well established that mechanical properties of concrete in general are adversely affected by high temperature exposure (Ref. 1 to 10). However, the effects of high temperature exposure on HPC's mechanical properties have been found to be more pronounced than the effects on conventional concrete. More importantly, when exposed to relatively rapid heating (above 1°C/min), HPC has been found to be more prone to spalling failure. Spalling failures in laboratory conditions have been characterized from being progressive (continuous spalling of small layers on the specimen's surface) to explosive (sudden disintegration of the specimen accompanied by the release of a large amount of energy which projects the broken concrete fragments with high velocity). It has been theorized that the higher susceptibility of HPC to explosive spalling at high temperature is due, in part, to its lower permeability, which limits the ability of water vapor to escape from the pores. This results in a build-up of vapor pressure within the concrete. As heating increases, the pore pressure also increases. This increase in vapor pressure continues until the internal stresses become so large as to result in sudden, explosive spalling. Spalling, however, has been observed on an inconsistent basis. Often, explosive spalling has occurred to only a few HPC specimens from a larger group of specimens that were subjected to identical testing conditions. This erratic behavior makes it difficult to predict with certainty under what conditions HPC will fail by explosive spalling.

NIST is conducting a multi-year research program that aims to develop a fundamental understanding of the effects of elevated temperature exposure on HPC performance and to quantify the influences of different concrete parameters on the spalling potential and engineering properties of HPC. This paper presents the results that deal with the residual mechanical properties of HPC exposed to elevated temperatures.

EXPERIMENTAL PROGRAM

This portion of the test program examines the effects of *w/cm* and the presence of silica fume on the residual properties and spalling tendency of HPC exposed to elevated temperatures.

All tests were performed under the *steady-state* temperature test condition following the test method shown in Figure 1. The concrete cylinder is heated without loading to a target temperature T using a constant ambient heating rate of 5 °C/min. The ambient temperature is then held constant for a period of time t_1 until a *steady-state* temperature condition has been reached in the specimen. The specimen is subsequently allowed to cool to room temperature and is loaded to failure in uniaxial compression. A "steady-state" temperature condition is defined as when the temperature at the center of the specimen is within 10 °C of the target temperature and the difference between the surface and center temperatures is less than 10 °C.

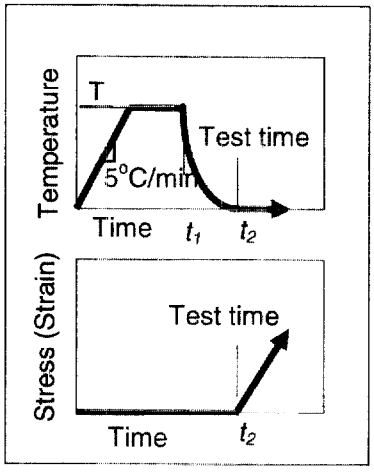

Figure 1. Residual property test method

All specimens were made using ASTM Type I portland cement, crushed limestone aggregate (13 mm nominal maximum size) with a fineness modulus (FM) of 5.40, natural sand with an FM of 2.85, silica fume, and a high range water-reducing admixture (HRWRA). The silica fume is in the form of a slurry with a density of 1.42 g/cm^3 and a 54 % silica fume concentration (by mass).

The specimens were made of four concrete mixtures, designated mixtures I to IV. Mixture I had the lowest *w/cm* of 0.22 and contained 10 % of silica fume by mass as cement replacement. Mixtures II and III had the same *w/cm* of 0.33, and were designed to have similar strength but differ by the inclusion of silica fume (mixture II contained 10 % of silica fume, while mixture III contained no silica fume). Mixture IV had the highest *w/cm* ratio of 0.57 and contained no silica fume. The mixture proportions and properties of fresh and hardened concrete are shown in Table 1. Initial moisture contents represent the amount of free water in the concrete and were obtained by drying small concrete samples (400-day old samples) at 105 °C until the difference in mass losses between measurements is negligible (≤ 0.1 %).

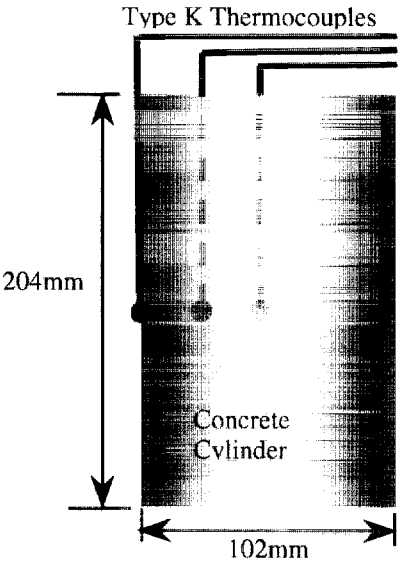

Figure 2. Specimen dimensions and instrumentation scheme

All test specimens were 102 mm by 204 mm cylinders. The specimens were cured under water at room temperature (nominally 23 °C) until close to test time. Two specimens from each concrete mixture were instrumented with three thermocouples to develop the internal temperature profiles on the cross section of the test specimens (see Figure 2) and establish the heating regimen. Dynamic elastic modulus was measured using the impact-resonance method in ASTM C 215. Compressive strengths were measured according to ASTM C 39 and the ends of the cylinders were ground flat prior to heating.

EXPERIMENTAL RESULTS

Table 2 summarizes the measurements of heat-induced mass loss and changes in dynamic elastic modulus and compressive strength of the test specimens. Measurement accuracy is expressed in terms of standard

deviation (SD) and coefficients of variation (CV), which are also listed in Table 2. The convention used in naming the test specimens is as follows:

Test Method - Concrete Mixture – Target Core Temperature – Specimen Number
(Residual Strength) (I to IV) (23 °C to 450 °C) (1, 2, 3...)

Table 1. Concrete Mixture Proportions and Properties

Materials and Properties	Mixture I (*w/cm*=0.22)	Mixture II (*w/cm*=0.33)	Mixture III (*w/cm*=0.33)	Mixture IV (*w/cm*=0.57)
Cement	595.9 kg/m^3	595.9 kg/m^3	661.6 kg/m^3	376.4 kg/m^3
Water	133.0 kg/m^3	198.6 kg/m^3	198.6 kg/m^3	213.0 kg/m^3
Coarse Aggregate	845.8 kg/m^3	845.8 kg/m^3	845.8 kg/m^3	853.8 kg/m^3
Fine Aggregate (*SSD*)	733.6 kg/m^3	733.6 kg/m^3	733.6 kg/m^3	868.2 kg/m^3
Silica Fume	65.7 kg/m^3	65.7 kg/m^3	0	0
HRWRA	400 ml/m^3	354 ml/m^3	154 ml/m^3	0
Fresh Concrete				
• Slump	235 mm	230 mm	35 mm	75 mm
• Air Content	3.2 %	2.8 %	2.0 %	2.5 %
Hardened Concrete				
• Initial Moisture Content	5.03 %	6.07 %	6.26 %	7.33 %
• Compressive Strength:				
28-day	75.3 MPa	66.0 MPa	53.2 MPa	40.6 MPa
58-day	86.7 MPa	79.5 MPa	58.9 MPa	41.9 MPa
400-day	92.5 MPa	87.9 MPa	75.5 MPa	50.6 MPa
• Dynamic Elastic Modulus				
58-day	34.4 GPa	37.2 GPa	36.7 GPa	34.4 GPa
400-day	47.2 GPa	43.7 GPa	44.1 GPa	36.7 GPa

Heating Behavior

Figures 3 and 4 provides information on temperature development and moisture (evaporated capillary pore water and chemically bound water) movement inside the concrete cylinders during heating to a target temperature of 450 °C. In Figure 3, the thick solid line represents the ambient temperature inside the furnace. The thin solid line is the temperature measured on the cylinder surface. The broken dashed line is the temperature at a point inside the cylinder, 25 mm from the surface (middepth). The dotted line is the temperature at the center of the cylinder, 51 mm from the surface.

Figure 4 shows the thermal gradient between the surface and center of the cylinder during heating. The first two vertical dashed lines from the left indicate perturbations in the rates of temperature rise between the surface and center of the cylinder (1 hr: 15 min and 1 hr: 55 min). These coincide with concrete temperatures at the center of the cylinders of slightly above 100 °C and approximately 205 °C, as indicated by the two vertical dashed lines at the same times on Figure 3. The perturbations in rates of temperature rise at surface and center of the cylinder are believed to be due to the rapid release of free water and chemically bound water at these two temperatures. At slightly above 100 °C, free water in the concrete begins to evaporate rapidly. A moisture front is driven by the heat toward the core of the specimen, causing a decrease in the rate of temperature rise at the specimen center and thus an increase in the thermal gradient between the specimen's surface and center. Beginning at approximately 205 °C, significant chemically-bound water is released. This caused a similar decrease in the rate of temperature rise at the core, as marked by the second dashed line in Figures 3 and 4. The thermal gradient between the

specimen surface and center reaches a maximum of 36 °C after 2 hr: 20 min of heating, at a corresponding center temperature of 270 °C. After this point, the rate of temperature rise on the surface begins to decrease faster than that of the core, causing the thermal gradient to decrease as shown in Figure 4. This trend continues until a true steady-state thermal condition develops after 4 hr of heating, when the surface-to-core thermal gradient is reduced to zero. After 5 hr:15 min of heating, the specimen core reaches the target temperature of 450 °C and is about 6 °C higher than the concrete surface.

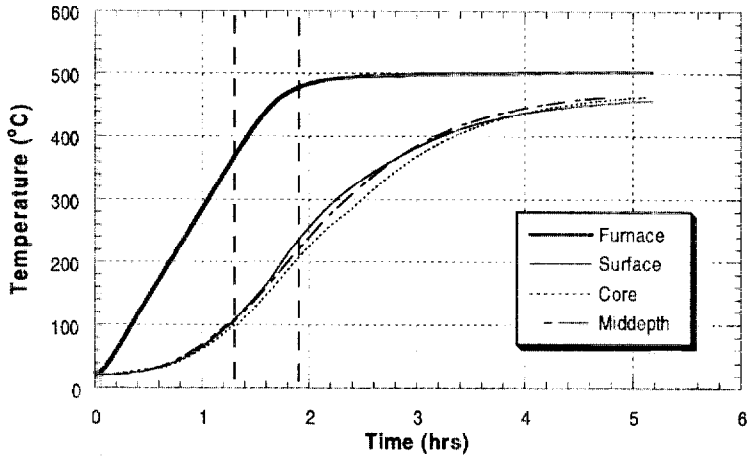

Figure 3. Temperature development inside mixture I cylinder

Heat-induced mass losses for all four concrete mixtures are shown in Figures 5 and 6. Figure 5 shows mass losses obtained from thermogravimetric analysis (TGA) of small samples (approximately 100 mg each) taken from the four concrete mixtures (ref. 10). Figure 6 shows mass losses obtained from heating full cylinders at 5 °C/min. The two vertical dashed lines in each figure indicate temperatures at which there were changes in rates of mass loss. The TGA results show that, beginning at slightly above 100 °C (first vertical dashed line in Figure 5), all four mixtures sustain similar temperature rates and amounts of mass loss. This coincides with the changes in the rates of temperature rise between the surface and center of the cylinder due to rapid removal of free water as discussed above (see Figure 3). A slower rate of mass loss begins at about 215 °C (second vertical dashed line in Figure 5) for all four concrete mixtures. While the mass loss rates were not significantly different for the four mixtures, the amounts of mass loss varied. Mixtures III and IV (*w/cm* = 0.33 and 0.57, respectively), which contained no silica fume, sustained similar but larger loss than mixtures I and II (*w/cm* = 0.22 and 0.33), which contained silica fume. As discussed above, the mass losses at this stage are due primarily to the release and evaporation of chemically bound water in the concrete samples. Figure 6 shows mean mass losses in the specimens. The results show that mass losses in mixture III and IV specimens follow the same two stages that begin at slightly above 100 °C and 200 °C as observed in the TGA measurements, with the mixture IV specimen sustaining the highest amount of mass loss. However, the changes in rate of mass loss for mixtures I and II at above 200 °C are less apparent, with the mixture I specimen sustaining no change in rate of mass loss up to 300 °C. It should be noted that mass loss data for mixture I specimens at 450 °C are not available due to explosive spalling of all three specimens while being heated to that target temperature. More detailed discussion concerning the explosive spalling of this group of specimens is given in the next section.

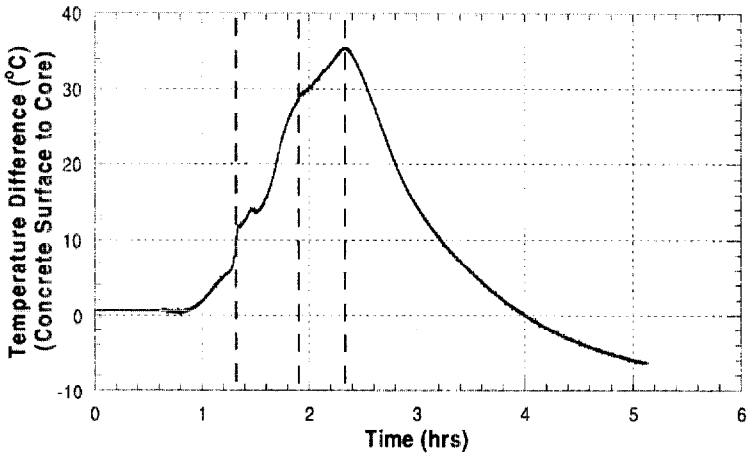

Figure 4. Thermal gradient between surface and core of mixture I cylinder

Recall that the initial free water moisture contents for the four concrete mixtures ranged between 5.0 % for mixture I and 7.3 % for mixture IV (see Table 1). The ranges of free water losses in all four concrete mixtures are represented by the horizontal band in Figures 5 and 6 (at normalized masses of 0.93 and 0.95). The TGA results, shown in Figure 5, indicate that all four mixtures sustained significant loss of free water and chemically bound water at about 215 °C (marked by the second vertical dashed line). However, the results of heating full-size specimens, shown in Figure 6, indicate that while specimens of mixtures II, III, and IV appear to lose most of this free water at 215 °C, the water in mixture I specimen was not completely lost at this temperature (only 4 % loss). Similarly, but to a lesser extent, the mixture II specimens also experienced a slightly more restrictive process of water loss (5.5 %) compared with the TGA result. These differences in mass loss between the TGA samples and the heated cylinders indicate that, while mixture III and IV cylinders have little problem losing water during heating to high temperatures, the silica fume containing mixture I and, to a lesser extent, mixture II cylinders will have a more restrictive water loss process and could thus develop significant internal pressures (leading to spalling).

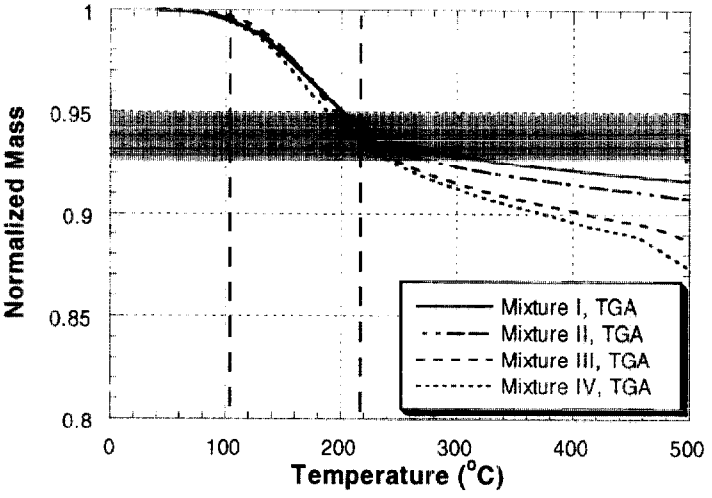

Figure 5. Mass losses from TGA

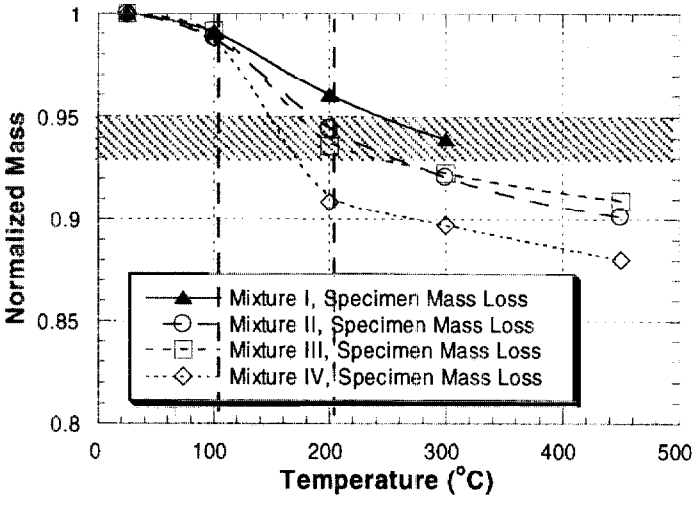

Figure 6. Mass losses from heating of full-size cylinders

Spalling Characteristics

As listed in Table 2, explosive spalling occurred during heating of five specimens, four of mixture I concrete and one of mixture II. Both mixtures I and II contained 10 percent of silica fume as cement replacement. Explosive spalling is characterized by the sudden disintegration of the specimens into fine fragments. This disintegration is accompanied by a sharp loud sound and the release of a large amount of energy that projects the small concrete fragments at high velocity in all directions. Reconstruction of the exploded specimens shows that the largest remaining piece in all cases is the concrete core, which measured approximately 70 mm at maximum width and 120 mm at maximum length. An approximately 20-mm thick outer shell of fragmented concrete surrounds this core. The depth of approximately 20 mm appears to be the location of the primary fracture surface. Figure 7 shows the fragments of an exploded specimen and a schematic of the cracking patterns in a reconstructed specimen.

Of the four exploded mixture I specimens, one belongs to a group of five specimens with a target temperature of 300 °C (specimen RS-I-300-2). This specimen exploded at 2 hr: 5 min into the heating

process, with the furnace temperature being maintained at 300 °C and the temperature at the center of the cylinder was 240 °C. The other three exploded mixture I specimens belong to the group of three specimens being heated to 450 °C (specimens RS-I-450-1 to 3). These specimens exploded when the centers of the cylinders reached temperatures ranging from 240 °C to at 280 °C. The exploded mixture II specimen (RS-II-300-4) belongs to the group being heated to 300 °C. This cylinder exploded when the temperature at its center reached 275 °C. The temperature range in which explosive spalling occurred in mixture I specimens is superposed on the temperature profile history (Figure 5) and thermal gradient history (Figure 6) as shown in Figures 8 and 9. As can be seen in Figure 9, the temperature range in which explosive spalling occurred coincides with the time when the maximum thermal gradient between the specimen surface and center occurred. This suggests that, while internal pore pressure may be the primary cause for the explosive spalling of the specimens, as evidenced by the high velocity with which the concrete fragments were projected at failure, the buildup of thermally induced strain energy was also at a maximum at this time, and thus thermal stress might have a secondary role in this failure.

Figure 7. Remnants of an exploded cylinder and rendering of the fracture formation

Residual Mechanical Properties

Compressive strengths of unheated (23 °C) and heated specimens, normalized with respect to the mean strengths of the unheated specimens, are plotted with respect to the target temperatures in Figure 10. The individual test data are shown by symbols and the means by lines. As shown in Figure 10, relative compressive strengths of mixtures III and IV concretes varied similarly with increasing temperature. The strength reduction in these two mixtures can be characterized by an initial strength reduction of between 25 % to 30 % at 100 °C. This is followed by no significant change in relative compressive strength between 100 °C to 300 °C. Further reduction in compressive strength occurs at temperatures above 300 °C. Exposure to 450 °C caused a 50 % loss in compressive strength for mixtures III and IV.

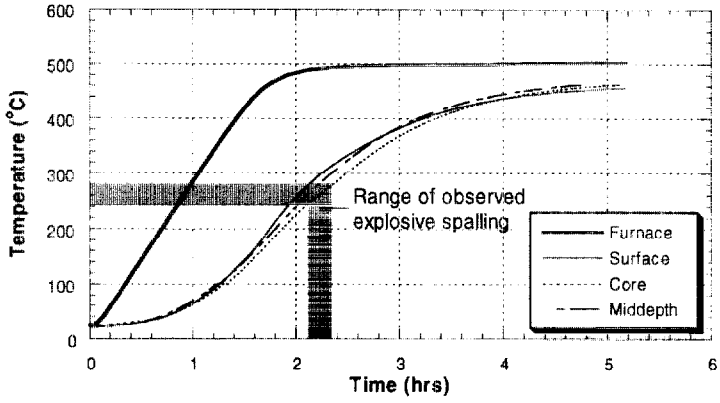

Figure 8. Temperature and time ranges of observed explosive spalling in mixture I specimens

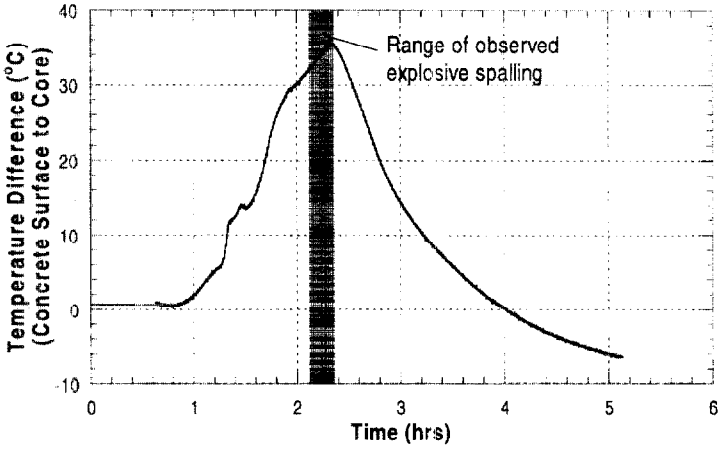

Figure 9. Range of thermal gradient when explosive spalling occurred

The concretes with silica fume, mixtures I and II, had similar strength reductions of between 10 % to 15 % at 100 °C. At temperatures above 100 °C, the relative strength of mixture II continued to drop - almost linearly - with increasing temperature, while mixture I experienced a strength recovery at temperatures between 100 °C and 200 °C. Between 200 °C and 300 °C, the relative strength of mixture I decreased at a similar rate as that of mixture II. However, mixture I sustained only 10 % to 20 % strength loss at 300 °C, while the strength loss for mixture II was at 30 % to 35 % at this temperature. At 450° C, mixture II sustained a similar amount of strength loss, about 50 %, as for mixtures III and IV. Analysis of variance shows that, at 100 °C, mixtures I and II had similar relative strength loss. This strength loss was less than that of mixtures III and IV. At 200 °C, mixture I had the least relative strength loss, while mixtures II, III, and IV sustained similar strength loss. This trend continued at 300 °C, with mixture III sustained a slightly less strength loss than mixtures II and IV. Compressive strength data for mixture I at 450 °C was not available due to explosive spalling of the entire group of specimens (RS-450-I-1 to 3). Data for mixtures II, III, and IV shows no different in relative strength at this temperature.

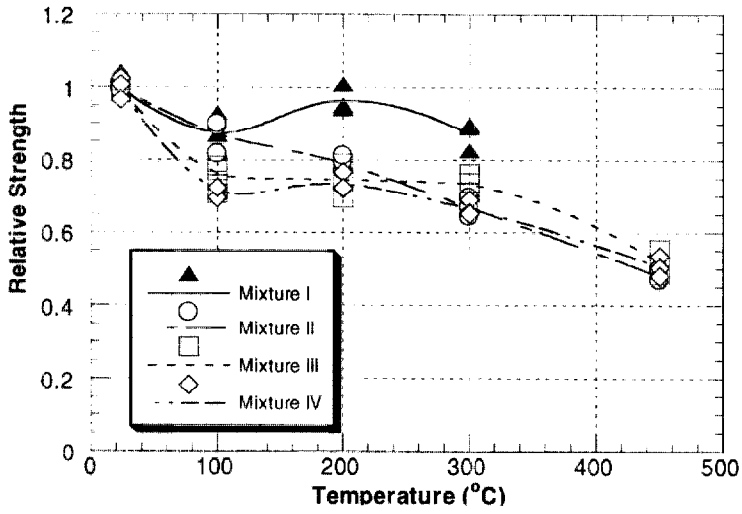

Figure 10. Residual relative compressive strength vs. temperature.

These results indicate that, within the ranges of original compressive strengths (51 MPa to 93 MPa) and *w/cm* ratios (0.22 to 0.57) studied in this program, concrete with higher original compressive strength, or lower *w/cm* ratio, experienced less relative strength loss due to high temperature exposure than concrete with lower original compressive strength. In concretes with similar *w/cm* ratio and strength (mixture II and III), the presence of silica fume appears to result in lower strength loss up to the temperature of 200 °C.

Figure 11 shows the variation of residual dynamic modulus of elasticity with increasing temperatures. The symbols in Figure 11 represent individual test data, and the lines represent the means. As shown in this figure, the relative dynamic modulus of elasticity of the four mixtures decreased similarly with increasing temperature. Between room temperature (23 °C) and 300 °C, the dynamic modulus of elasticity for all mixtures decreased by more than 50 %. Between 300 °C to 450 °C, the rate of elastic modulus reduction decreased.

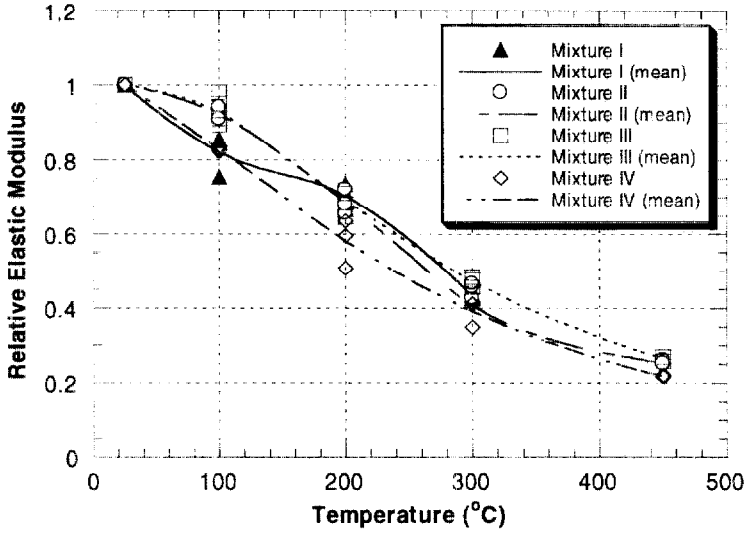

Figure 11. Residual relative dynamic modulus of elasticity vs. temperature

Mixtures II and III, which have similar room-temperature compressive strengths (81 MPa and 72 MPa, respectively), display

Table 2. Summary of test results

	Test Name	Mass Loss (%)	SD/CV (%) of Mass Loss	E_{dyn} Before Heating (Pa)	E_{dyn} After Heating (Pa)	Residual E_{dyn} (%)	SD/CV (%) of Residual E	Test Strength (MPa)	Residual Strength (%)	SD/CV (%) of Residual Strength	Spalling
Mixture I	RS-I-25-1	0.00		4.73E+10		100.0		90.56	100.0	3.6/3.6	
	RS-I-25-2	0.00		4.71E+10		100.0		90.60	100.0		
	RS-I-25-3	0.00		4.71E+10		100.0		96.40	100.0		
	RS-I-100-1	1.02	.14/15.8	4.60E+10	3.47E+10	75.5	5.8/7.0	75.64	81.8	5.5/6.4	
	RS-I-100-2	0.75		4.41E+10	3.76E+10	85.2		80.34	86.8		
	RS-I-100-3	0.84		4.24E+10	3.63E+10	85.7		85.92	92.9		
	RS-I-200-1	4.38	.41/10.5	4.46E+10	2.98E+10	66.7	3.5/5.0	93.29	100.8	3.6/3.8	
	RS-I-200-2	3.57		4.68E+10	3.45E+10	73.6		87.84	94.9		
	RS-I-200-3	3.85		4.67E+10	3.34E+10	71.4		87.08	94.1		
	RS-I-300-1	6.19	.11/1.7	4.61E+10	2.02E+10	43.8	0.6/1.4	82.85	89.5	3.8/4.4	
	RS-I-300-2			4.70E+10							YES
	RS-I-300-3	6.02		4.54E+10	1.97E+10	43.3					
	RS-I-300-4	6.07		4.71E+10	2.00E+10	42.4		76.41	82.6		
	RS-I-300-5	5.94		4.72E+10	2.05E+10	43.5		82.19	88.8		
	RS-I-450-1			4.81E+10							YES
	RS-I-450-2			4.65E+10							YES
	RS-I-450-3			4.59E+10							YES
Mixture II	RS-II-25-1	0.00		4.32E+10		100.0		88.87	100.0	0.9/0.9	
	RS-II-25-2	0.00		4.39E+10		100.0		87.66	100.0		
	RS-II-25-3	0.00		4.40E+10		100.0		87.31	100.0		
	RS-II-100-1	1.22	.07/5.8	4.25E+10	3.94E+10	92.6	1.6/1.7	78.53	89.3	4.6/5.3	
	RS-II-100-2	1.13		4.17E+10	3.92E+10	94.1		79.11	90.0		
	RS-II-100-3	1.09		4.36E+10	3.97E+10	91.0		71.78	81.6		
	RS-II-200-1	6.03	.48/8.6	4.34E+10	2.86E+10	65.8	3.2/4.6	67.75	77.0	2.0/2.6	
	RS-II-200-2	5.08		4.29E+10	3.10E+10	72.1		69.84	79.4		
	RS-II-200-3	5.55		4.37E+10	2.98E+10	68.1		71.32	81.1		
	RS-II-300-1	8.09	.15/1.8	4.40E+10	1.88E+10	42.8	2.0/4.5	58.84	66.9	2.6/3.9	
	RS-II-300-2	7.80		4.31E+10	1.98E+10	45.9		56.62	64.4		
	RS-II-300-3	7.91		4.30E+10	2.00E+10	46.6		61.22	69.6		
	RS-II-300-4										YES
	RS-II-450-1	9.16	1.1/11.4	4.36E+10	1.13E+10	26.0	0.5/2.1	41.32	47.0	1.5/3.3	
	RS-II-450-2	9.30		4.50E+10	1.12E+10	25.0		43.78	49.8		
	RS-II-450-3	11.17		4.36E+10	1.10E+10	25.2		41.40	47.1		
Mixture III	RS-III-25-1	0.00		4.41E+10		100.0		75.43	100.0	1.5/1.5	
	RS-III-25-2	0.00		4.34E+10		100.0		76.54	100.0		
	RS-III-25-3	0.00		4.48E+10		100.0		74.23	100.0		
	RS-III-100-1	0.83	.12/13.9	4.20E+10	3.85E+10	91.8	3.9/4.2	58.12	77.1	3.4/4.5	
	RS-III-100-2	0.69		4.13E+10	4.06E+10	98.4		55.94	74.2		
	RS-III-100-3	0.88		4.05E+10	3.88E+10	95.8		59.08	78.4		
	RS-III-100-4	0.97		4.25E+10	3.80E+10	89.4		53.31	70.7		
	RS-III-200-1	6.73	.29/4.5	4.33E+10	2.80E+10	64.6	4.0/5.7	59.58	79.0	4.7/6.4	
	RS-III-200-2	6.18		4.25E+10	3.05E+10	71.8		52.47	69.6		
	RS-III-200-3	6.30		4.19E+10	2.98E+10	71.0		56.73	75.2		
	RS-III-300-1	8.09	.30/3.9	4.24E+10	1.94E+10	45.7	1.4/2.9	55.54	73.7	2.7/3.6	
	RS-III-300-2	7.54		4.31E+10	2.08E+10	48.3		57.52	76.3		
	RS-III-300-3	7.61		4.36E+10	2.08E+10	47.7		53.50	70.9		
	RS-III-450-1	9.31	.45/4.9	4.33E+10	1.16E+10	26.9	0.6/2.2	41.75	55.4	3.4/6.6	
	RS-III-450-2	8.54		4.50E+10	1.17E+10	25.9		36.60	48.5		
	RS-III-450-3	9.31		4.33E+10	1.16E+10	26.9		38.72	51.3		
Mixture IV	RS-IV-25-1	0.00		3.67E+10		100.0		51.91	100.0	3.0/3.0	
	RS-IV-25-2	0.00		3.67E+10		100.0		51.03	100.0		
	RS-IV-25-3	0.00		3.67E+10		100.0		48.97	100.0		
	RS-IV-100-1	1.33	.24/21.1	3.72E+10	3.05E+10	82.2	0.7/0.8	35.21	69.5	1.6/2.3	
	RS-IV-100-2	0.88		3.70E+10	3.10E+10	83.6		35.16	69.4		
	RS-IV-100-4	1.27		3.75E+10	3.11E+10	82.9		36.58	72.2		
	RS-IV-200-1	9.53	.34/3.7	3.65E+10	1.85E+10	50.7	6.6/11.4	38.82	76.7	2.6/3.6	
	RS-IV-200-2	8.96		3.65E+10	2.32E+10	63.6		36.45	72.0		
	RS-IV-200-3	8.94		3.73E+10	2.22E+10	59.5		36.58	72.2		
	RS-IV-300-1	9.59	.92/9.0	3.66E+10	1.27E+10	34.8	3.6/9.3	34.91	68.9	2.1/3.2	
	RS-IV-300-2	9.93		3.70E+10	1.53E+10	41.2		33.15	65.5		
	RS-IV-300-3	11.33		3.67E+10	1.50E+10	41.0		32.96	65.1		
	RS-IV-450-1	11.96	.35/2.9	3.67E+10	7.96E+09	21.7	0.3/1.5	27.06	53.4	2.8/5.4	
	RS-IV-450-2	12.30		3.63E+10	7.84E+09	21.6		25.46	50.3		
	RS-IV-450-3	11.61		3.74E+10	8.29E+09	22.2		24.29	48.0		

almost identical residual dynamic modulus of elasticity. The reduction in modulus of mixtures II and III concretes are consistently less (5 % to 10 %) than that of mixture IV, which has a room-temperature compressive strength of 47 MPa. The reduction in dynamic modulus of elasticity for mixture I (*w/cm*=0.22, 98MPa) is less consistent within the range of temperatures examined.

SUMMARY AND DISCUSSIONS

This study examined the effects of exposure to temperatures up to 450 °C on the heating behavior, potential for explosive spalling, and residual mechanical properties of four HPC mixtures. The following summarizes experimental results and observations:

- The combination of low *w/cm* (0.33 or less) and silica fume appears to increase the potential for explosive spalling in unstressed residual strength tests. The temperatures at the center of the cylinders when explosive spalling occurred were in the range of 240 °C to 280 °C, slightly beyond the temperatures at which much of the chemically bound water has already been released from the concrete matrix.
- Evidence of a more restricted mass loss process in the cylinders that exploded, coupled with the violent fragmentation of the cylinders, further support the hypothesis that internal pore pressure buildup is the primary cause for explosive spalling. However, the fact that explosive spalling occurred when the maximum thermal gradient also existed in the specimen implies that the buildup of strain energy due to thermal stress might have a secondary role in the explosive spalling mechanism. Whether this secondary role is to delay or to contribute to explosive spalling remains to be quantified (since the aggregates expand with increasing temperature while the cement paste contracts).
- Within the ranges of original compressive strengths (51 MPa to 93 MPa) and *w/cm* (0.22 to 0.57) examined in this test program, HPC with higher original compressive strength, or lower *w/cm* ratio, sustained lower relative strength loss due to high temperature exposure than those with lower original compressive strength. In HPC with similar *w/cm* and strength (mixture II and III), the presence of silica fume appears to result in lower strength loss up to the temperature of 200 °C.
- Dynamic modulus of elasticity of the four HPC mixtures in this test program decreased similarly with increasing temperature. Between room temperature (23 °C) and 300 °C, the dynamic modulus of elasticity for all mixtures decreased by more than 50 %. Between 300 °C to 450 °C, the rate of modulus reduction decreased.

REFERENCES

1 Schneider, U.; "Properties of Materials at High Temperatures - Concrete", RILEM - Committee 44 - PHT, University of Kassel, Kassel, June, 1985.

2 Phan, L.T.; Carino, N.J.; Duthinh, D.; Garboczi, E., "NIST International Workshop on Fire Performance of High Strength Concrete, NIST, Gaithersburg, MD, February 13-14, 1997 – Proceedings," NIST SP 919, Gaithersburg, Maryland, September1997.

3 Castillo, C.; Durrani, A. J., "Effect of transient high temperature on high-strength concrete," ACI *Materials Journal*, v.87, n.1, 1990, pp. 47-53.

4 Hertz K., "Danish Investigations on Silica Fume Concretes at Elevated Temperatures," Proceedings of ACI 1991 Spring Convention, March 17-21.

5 Sullivan, P. J. E.; Shanshar, R., "Performance of concrete at elevated temperatures (as measured by the reduction in compressive strength," Fire Technology, v. 28, n. 3, Aug 1992, pp. 240-250.

6 Abrams, M.S., "Compressive Strength of Concrete at Temperatures to 1600°F," ACI SP 25, Temperature and Concrete, Detroit, Michigan, 1971.

7 Furumura, F.; Abe, T.; Shinohara, Y.; "Mechanical Properties of High Strength Concrete at High Temperatures," Proceedings of the Fourth Weimar Workshop on High Performance Concrete: Material Properties and Design, Weimar, Germany, October 4th and 5th, 1995, pp. 237 - 254.

8 Felicetti, R.;Gambarova, P.G.; Rosati, G.P.; Corsi, F.; Giannuzzi, G.; "Residual Mechanical Properties of HSC Subjected to High-Temperature Cycles," Proceedings, 4th International Symposium on Utilization of High-Strength/High-Performance Concrete, Paris, France,1996, pp. 579-588.

9 Phan, L.T., "Fire Performance of High-Strength Concrete: A Report of the State of the Art," NISTIR 5934, National Institute of Standards and Technology, Gaithersburg, Maryland 20899, December 1996.

10 Bentz, D.P., "Fibers, Percolation, and Spalling of High Performance Concrete," accepted by ACI Materials Journal, 2000.